References

[1] Bird, R. B., "Unsteady Pseudoplastic Flow Near a Moving Wall," *AIChE Journal*, Vol. 5, No. 4, Dec. 1959, p. 565.

[2] Wells, C. S., Jr., "Unsteady Boundary Layer Flow of a Non-Newtonian Fluid on a Flat Plate," *AIAA Journal*, Vol. 2, No. 5, May 1964, pp. 951–952.

[3] Rott, W., "Laminare Strömung dilatanter Flüssigkeiten in der Nähe einer plötzlich in Bewegung gesetzen Platte," *Chemical Engineering Science*, Vol. 26, 1971, pp. 739–742.

[4] Chen, T. Y. W. and Wollersheim, D. E., "Solution of Unsteady Flow of Power Law Fluids," *AIAA Journal*, Vol. 10, No. 5, May 1972, pp. 689–691.

[5] Roy, S., "Contribution in Unsteady Flow of Power Law Fluids," *AIAA Journal*, Vol. 11, No. 2, Feb. 1973, pp. 238–239.

[6] Roy, S., "Diffusion in a Time-Dependent Three-Dimensional Boundary Layer," *Indian Journal of Physics*, Vol. 46, 1972, pp. 370–378.

[7] Shah, M. J., Ph.D. thesis, 1961, Univ. of California at Berkeley, Berkeley, Calif.

Stability Analysis of Cylinders with Circular Cutouts

B. O. ALMROTH,* F. A. BROGAN,† AND M. B. MARLOWE‡

Lockheed Palo Alto Research Laboratory, Palo Alto, Calif.

Nomenclature

X, θ	= shell surface coordinates
X, Y, Z	= Cartesian coordinates
R	= cylinder radius
h	= cylinder thickness
a	= cutout dimension (see Fig. 3)
F	= function [Eq. (2)]
w	= lateral displacement
N	= axial stress resultant
P	= applied axial load
N_0	= critical value of stress resultant
P_0	= critical value of axial load
$\bar{w}$	= w/h
$\bar{N}$	= N/N_0
$\bar{P}$	= P/P_0
α	= $a/(Rh)^{1/2}$

AN analysis is presented for the stability of axially compressed cylinders with circular cutouts. The numerical analysis was based on an extension of the finite-difference method which removes the requirements that displacement components be defined in the directions of the grid lines. The results from the nonlinear analysis are found to be in good agreement with previously available experimental results.

For shells of general shape and for shells of revolution whose symmetry has been destroyed by cutouts or local stiffening, loss of stability usually occurs by collapse at a limit load point. In such cases, stability analyses based upon the assumption of bifurcation from a linear prestress may be of little practical significance[1]; hence, to establish a meaningful collapse load for the shell, we must solve numerically a set of nonlinear partial differential equations. However, this approach leads to a massive computational effort, and only recently has it been possible to obtain solutions in agreement with test results for the collapse of shells with cutouts.

Received May 10, 1973. This work was sponsored in part by the Lockheed Independent Research Program and in part under Contract NAS1-10843 with NASA/Langley Research Center.

Index category: Structural Stability Analysis.

* Senior Staff Scientist. Member AIAA.

† Research Scientist.

‡ Research Scientist. Member AIAA.

Although significant progress has been made in numerical techniques, the primary reason for the recent expansion of structural analysis capabilities is the rapid increases in computer technology. Indeed, the work reported here could not have been performed without modern high speed scientific computers such as the Control Data Corporation CDC 6600 and CDC 7600.

A collapse analysis for axially compressed cylindrical shells with rectangular cutouts was first presented in 1970 (Ref. 2). Results for similar, but thinner, cylinders were compared with experimental results in Ref. 3. It was found in this investigation that the influence of a cutout on the collapse load could be established with good accuracy by use of the STAGS computer code. This code is based upon the finite-difference energy method discussed in Refs. 4 and 5. The version of STAGS with which the results of Ref. 3 were obtained[6] is too restricted to handle efficiently shells with nonrectangular cutouts; hence, extensive modifications to the code were made before it was applied to shells with circular cutouts.

In the finite-difference energy method, as applied to shell analysis, the shell surface is divided into several area elements. At one point within each of these area elements, the displacements and their derivatives are expressed in terms of the displacement components at a number of points that may be selected independently. We shall here refer to the latter as grid points and to the points at which the energy is expressed as integration points. Through numerical integration over the integration points, the total potential energy of the system is expressed in terms of the discrete values of the displacement components at the grid points. Equilibrium configurations are found through minimization of the potential energy with respect to these free parameters.

The relations by which the displacements and their derivatives are expressed at the integration points in terms of the displacements at the grid points are referred to as finite-difference expressions. Traditionally, finite-difference methods for solution of the partial differential equations governing the behavior of thin shells have been applied in a rather restricted way. Although the method has been presented in text books in a more general form,[7] applications generally have been restricted to cases in which the grid is generated on a rectangular mapping of the shell surface, and grid and integration points are identical, being defined at intersections of coordinate lines.

The essence of the generalization presented here is that the directions of the displacement components need not coincide with the direction of the grid lines. There are no restrictions on the procedure that generates the grid points on the shell surface, but for practical reasons, it should provide a suitable numbering system for the grid points. Similar extensions have been suggested previously and applied in linear analysis.[8,9] In both these cases, the finite-difference approximations were derived by use of Green's Theorem, while in the present analysis they are based on a Taylor series expansion.

A suitable grid for a cylinder with a circular cutout can be generated by the functions

$$\begin{aligned} X &= R \sin [F(\cos\theta)/R] \\ Y &= R \cos [F(\cos\theta)/R] \\ Z &= F \sin\theta \end{aligned} \tag{1}$$

where R is the radius of the cylinder and X, Y, Z are the Cartesian coordinates of a point on the cylinder (Z is measured in the axial direction). The surface coordinates are denoted by θ and x and $F(x)$ is defined by

$$F = \{[(a(1-x)+\tfrac{1}{2}\pi Rx)\sin\theta]^{2/(1-x)} + [(a(1-x)+Lx)\cos\theta]^{2/(1-x)}\}^{(1-x)/(2)} \tag{2}$$

where a is the radius of the cutout and L is the half length of the cylinder. A computer generated picture of $\frac{1}{8}$ of a cylinder with its surface grid is shown in Fig. 1.

For cylinders with rectangular cutouts, it was shown in Ref. 3 that theoretical results could be obtained which were in very good agreement with results from experimental analysis. The

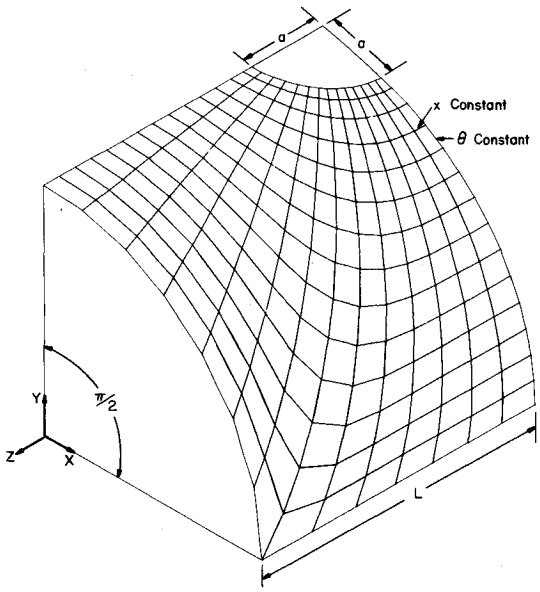

Fig. 1 Finite-difference grid for cylinder with circular cutout.

numerical analysis presented here is primarily intended to establish a similar agreement between test and theory for cylinders with circular cutouts. Examples have been chosen which provide as much general information as possible about the behavior of cylinders with cutouts. A few cylinders with square cutouts were analyzed for the purpose of comparison.

The dimensions and properties of the cylinders in the analysis were chosen so that comparisons could be made with the experimental results obtained by Starnes. The test results reported by Starnes[10] were for cylinders with one cutout, and the load was applied through the center of one of the end plates. Because this end plate was allowed to rotate, the prevailing boundary conditions were complicated. However, Starnes also ran a series of tests on cylinders with two diametrically opposed cutouts. In these cases, the boundary conditions corresponded to a uniform axial displacement of the shell edge. This type of boundary condition is not only easier to define in the theoretical analysis but it also allows for the use of an additional symmetry plane and, thus, a less expensive analysis. Consequently, the cylinders in this analytical study have two cutouts. All parameters were held constant except the shell thickness and the cutout radius (half the side for square cutouts). The fixed parameters were $R = 4$ in., $L = 10$ in., $E = 10^7$ psi, $\nu = 0.3$.

It was found, from experimental results[10] that the parameter

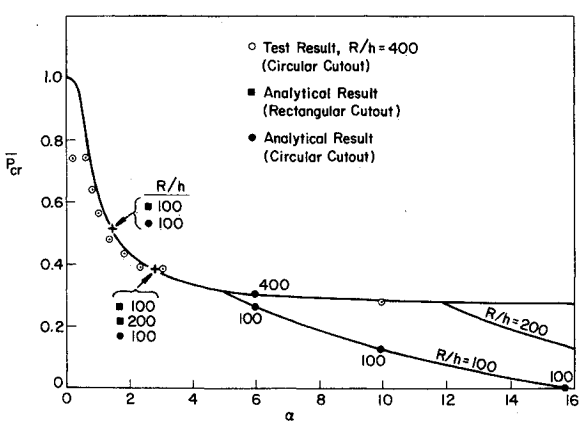

Fig. 2 Critical loads, theoretical and experimental.

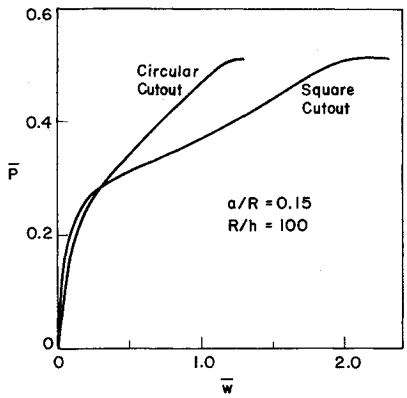

Fig. 3 Load displacement curves, $\alpha = 1.5$.

$\alpha = a/(Rh)^{1/2}$ determines the shell behavior. This conclusion is verified here by the theoretical analysis of cylinders with relatively small cutouts. The graphs depicting the normalized displacement $\bar{w}$ vs the normalized axial load $\bar{P}$ were found to be identical for one cylinder with $a/R = 0.15$, $R/h = 100$ and one with $a/R = 0.2121$, $R/h = 200$; i.e., $\alpha = 1.5$ for both. We notice, however, that for cylinders with sufficiently large cutouts, the value of α cannot alone determine the behavior of the shell. With two cutouts, for example, the critical load must be zero when $a/R = \pi/2$. This will occur, if $R/h = 100$ at $\alpha = 5\pi$ and if $R/h = 400$ at $\alpha = 10\pi$. Therefore, for cylinders with relatively large cutouts, there must be separate curve branches for different R/h values in the P_{CR} vs α diagram. This was found to be the case when the critical loads were compared for two cylinders with $\alpha = 6$. The cylinder with $a/R = 0.3$ and $R/h = 400$ carries a significantly larger axial load (normalized) than the one with $a/R = 0.6$ and $R/h = 100$.

All the results obtained from the analysis with uniform end shortening are shown in Fig. 2 together with a curve based on these computed data and the obvious location of the end points of the curves. The test data provided by Starnes are also plotted in the figure, and it appears that experimental and theoretical results are in very good agreement. It may be noticed also that virtually the same critical load is obtained whether the cutout is circular or square. Figure 3 shows the outward displacement at the cutout edge (midlength) as a function of the applied axial load for two cylinders with $\alpha = 1.5$, one with a circular and one with a square cutout. Similar results for two cylinders with $\alpha = 3.0$ are shown in Fig. 4.

The result that a cylinder with a square cutout can carry as high a load as a cylinder with a circular cutout is somewhat unexpected. It seems that the larger displacements at the edge of the square cutout results in more redistribution of the stresses. With the less favorable condition of uniform stress applied at the shell edge, it appears that shells with circular cutouts should

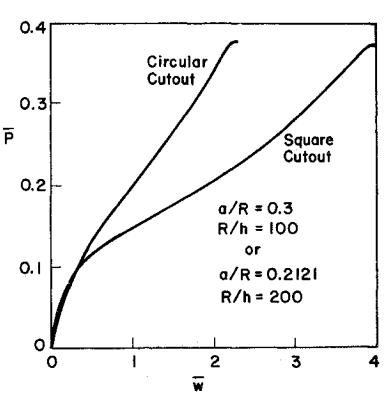

Fig. 4 Load displacement curves, $\alpha = 3.0$.

Table 1 Collapse loads

$R/h = 100$

Cutout		Critical load $\bar{P}$, with	
Type	Size, a/R	Unif. load	Unif. displacement
Circ.	0.6	0.236	0.510
Circ.	1.2	0.149	0.376
Circ.	2.4	0.035	0.303
Square	1.2	0.110	0.378

carry more load than those with square cutouts. A few cases were also analyzed with this loading condition, and the results are shown in Table 1. It can be seen that for this condition the critical loads are lower, especially for shells with square cutouts.

References

[1] Almroth, B. O. and Brogan, F. A., "Bifurcation Buckling as an Approximation of the Collapse Load for General Shells," *AIAA Journal*, Vol. 10, No. 4, April 1972, p. 463.

[2] Brogan, F. A. and Almroth, B. O., "Buckling of Cylinders with Cutouts," *AIAA Journal*, Vol. 8, No. 2, Feb. 1970, pp. 236–240.

[3] Almroth, B. O. and Holmes, A. M. C., "Buckling of Shells with Cutouts, Experiment and Analysis," *International Journal of Solids and Structures*, Vol. 8, 1972, p. 1057.

[4] Bushnell, D., Almroth, B. O., and Brogan, F. A., "Finite-Difference Energy Method for Nonlinear Shell Analysis," *Computers & Structures*, Vol. 1, 1972, pp. 361–387.

[5] Bushnell, D., "Finite Difference Energy Models Versus Finite Element Models—Two Variational Approaches in One Computer Program," *Proceedings of ONR Symposium on Numerical and Computer Methods in Structural Mechanics*, Academic Press, New York, to be published.

[6] "User's Manual for STAGS Computer Code," D266611, April 1972, Lockheed Missiles & Space Co., Sunnyvale, Calif.

[7] Collatz, L., *Functional Analysis and Numerical Mathematics*, Academic Press, New York, 1966.

[8] Budiansky, B. and Anderson, D. G. M., "Numerical Shell Analysis—Nodes Without Elements," presented at the 12th International Congress of Applied Mechanics, Stanford, Calif., Aug. 1968.

[9] Johnson, D. E., "A Difference-Based Variational Method for Shells," *International Journal of Solids & Structures*, Vol. 6, 1970, p. 699.

[10] Starnes, J. H., Jr., "The Effect of a Circular Hole on the Buckling of Cylindrical Shells," Ph.D. thesis, 1970, California Inst. of Technology, Pasadena, Calif.

Shooting Method for Solution of Boundary-Layer Flows with Massive Blowing

TSONG-MOU LIU* AND PHILIP R. NACHTSHEIM†

NASA Ames Research Center, Moffett Field, Calif.

Introduction

IN an earlier publication, Nachtsheim and Green[1] (1971) presented a numerical method to solve the boundary-layer equations with massive blowing. The method is based on bidirectional shooting starting from the dividing streamline. Recently, Liu and Nachtsheim[2] proved that, in the case of massive blowing, the parasitic eigenvalues associated with the boundary-layer equations equal the stream function with opposite sign and therefore are positive. The nonexistence of the negative parasitic eigenvalue guarantees that the backward shooting technique employed in Ref. 1 is stable. However, there is one drawback in Ref. 1, i.e., one cannot specify the blowing rate f_w and the wall temperature s_w a priori. This Note will present a modified shooting method to solve boundary-layer equations with massive blowing for specified f_w and s_w.

Received May, 1973.

Index category: Boundary Layers and Convective Heat Transfer—Laminar.

* Research Associate.

‡ Assistant Chief, Thermal Protection Branch.

Method Description

For boundary-layer flows with blowing, the stream function f is negative near the wall and positive at the edge and there is a dividing streamline where the oncoming flow is stopped by the injected flow and $f(\eta_0) = 0$. For massive blowing, the location of the dividing streamline increases with blowing rate and becomes very large. In the inner region, $\eta < \eta_0$, the parasitic eigenvalues of the equations are positive and large,[2] and it is wise not to integrate the equations from the wall (unstable direction), but instead one should integrate backward from the dividing streamline (stable direction) as in Ref. 1. This is the key point for the stable numerical integration of the massively blown boundary-layer equations.

The modification of the shooting method of Ref. 1 is illustrated as follows. Consider the Cohen-Reshotko equations

$$f''' + ff'' + \beta(1 + s - f'^2) = 0 \tag{1}$$

$$s'' + fs' = 0 \tag{2}$$

$$f(0) = -C, \quad f'(0) = 0, \quad s(0) = s_w \tag{3}$$

$$f'(\infty) = 1, \quad s(\infty) = 0 \tag{4}$$

This is the same set of equations considered in Ref. 1. Introduce a new independent variable

$$\zeta = (\eta - \eta_0)/\eta_0 \tag{5}$$

so that the wall is always located at $\zeta = -1$ and the dividing streamline is always located at $\zeta = 0$. This transformation avoids the difficulty of imposing wall conditions when η_w (in the notations of Ref. 1) is unknown a priori. The same idea has been applied successfully by Liu and Libby[3] to solve the flame sheet model for stagnation point flows. With this transformation, the location of the dividing streamline η_0 will appear as an unknown parameter in the conservation Eqs. (1) and (2). Moreover, to avoid confusion, new dependent variables are defined as follows:

$$F(\zeta) = f(\eta), \quad g(\zeta) = s(\eta) \tag{6}$$

Substituting Eqs. (5) and (6) into Eqs. (1) to (4), we obtain the following:

$$F''' + \eta_0 FF'' + \beta[\eta_0^3(1 + g) - \eta_0 F'^2] = 0 \tag{7}$$

$$g'' + \eta_0 Fg' = 0 \tag{8}$$

$$F(-1) = -C, \quad F'(-1) = 0, \quad g(-1) = s_w \tag{9}$$

$$F'(\infty) = \eta_0, \quad g(\infty) = 0 \tag{10}$$

$$F(0) = 0 \tag{11}$$

In this new set of equations, η_0 appears as a parameter that must be determined in the course of solution. We note that Eqs. (7–11) are a three-point, boundary-value problem; the additional boundary condition (11) is just the definition of the dividing streamline. Next, we generalize the automated procedure of Nachtsheim and Swigert[4] for satisfying the asymptotic boundary conditions at the outer edge of the boundary layer. Let

$$x_1 = F'(0), \quad x_2 = F''(0), \quad x_3 = g(0), \quad x_4 = g'(0) \tag{12}$$

where x_i, $i = 1, 2, 3, 4$, and η_0 must be chosen so that conditions (9) and (10) are satisfied. Differentiating Eqs. (7) to (8) with respect to x_i and η_0, we obtain the following perturbation equations:

$$F_{x_i}''' + \eta_0[FF_{x_i}'' + F''F_{x_i} + \beta(\eta_0^2 g_{x_i} - 2F'F_{x_i})] = 0 \tag{13}$$

$$g_{x_i}'' + \eta_0[Fg_{x_i}' + g'F_{x_i}] = 0 \tag{14}$$